INNERVAZIONE CARDIACA: SCINTIGRAFIA CON ^{123}I-METAIODOBENZILGUANIDINA (MIBG)

L'imaging scintigrafico con ^{123}I-MIBG è una delle poche metodiche disponibili in grado di valutare a livello pre-sinaptico la funzione simpatica cardiaca, che gioca un ruolo rilevante nel mantenimento della stabilità emodinamica e elettrofisiologica e che risulta alterata in varie condizioni cardiache quali lo scompenso cardiaco, le aritmie e la cardiopatia ischemica.

Il referto dovrà contenere una prima parte in cui saranno riportati: a) i dati anagrafici del paziente, le eventuali co-morbidità, i fattori di rischio, gli eventuali interventi cardiaci; b) il quesito diagnostico; c) la procedura, il tracciante utilizzato e l'attività somministrata.

Segue la descrizione dei risultati dell'esame scintigrafico che dovrà contenere una valutazione delle immagini planari e delle immagini SPECT. Sulle immagini planari sarà effettuata sia una analisi visuale che dovrà contenere la valutazione del grado di captazione miocardica globale del tracciante espressa in termini di "normale" / "anormale", sia una analisi semi-quantitativa, effettuata tracciando delle regioni di interesse su mediastino superiore e cuore sulle immagini planari precoci e tardive, ottenendo in tal modo dei parametri numerici che sono il rapporto cuore/mediastino (H/M) precoce e tardivo ed il wash-out rate (WR). Sulle immagini SPECT verrà effettuata una valutazione visuale del pattern di captazione espresso in termini di "captazione omogenea", "anomalie diffuse di captazione" o "anomalie segmentarie di captazione"; dovranno elencarsi i segmenti cardiaci sedi di anomalie di captazione utilizzando il modello a 17 segmenti (Cerqueira MD et al. Standardized myocardial segmentation and nomenclature for tomographic imaging of the heart. A statement for healthcare professionals from the Cardiac Imaging Committee of the Council on Clinical Cardiology of the American Heart Association. Circulation 2002; 105) ed indicarne la loro estensione e severità. Utilizzando uno score semi-quantitativo a 5 punti (0= captazione normale; 1= lieve riduzione della captazione; 2= moderata riduzione della captazione; 3= severa riduzione della captazioen; 4= assente captazione) sarà possibile esprimere l'uptake segmentario del tracciante e riportare un *defect score* globale, che sarà dato dalla somma di tutti gli score segmentari di captazione del tracciante. Nel caso in cui il paziente abbia effettuato anche uno studio di perfusione miocardica sarà utile inserire il confronto tra i due studi.

Il referto, infine, dovrà terminare con le conclusioni dell'esame scintigrafico che dovranno descrivere: a) la normale/ridotta distribuzione del tracciante; b) se i valori di H/M precoci e tardivi risultino significativamente ridotti e i valori di WR elevati (che indicano un accelerato washout del tracciante dalla terminazione nervosa pre-sinaptica), parametri che indicano la presenza di una terminazione nervosa simpatica

disfunzionante. Si dovrà descrivere la presenza di un match/mismatch con l’esame di perfusione cardiaca (qualora effettuato), dal momento che la presenza di un mismatch (cioè studio di perfusione normale e studio di innervazione anormale) si traduce in una zona del miocardio ad elevata eterogeneità elettrica e quindi più suscettibile a sviluppare aritmie fatali.

Clin Transl Imaging (2015) 3:357–363
DOI 10.1007/s40336-015-0143-x

REVIEW ARTICLE

^{123}I-Metaiodobenzylguanidine cardiac innervation imaging: methods and interpretation

T. Pellegrino[1] · V. Piscopo[2] · M. Petretta[3] · A. Cuocolo[2]

Received: 23 July 2015 / Accepted: 11 September 2015 / Published online: 23 September 2015

Abstract The heart is richly innervated with sympathetic and parasympathetic fibers that work in conjunction with norepinephrine to accurately preserve hemodynamic and electrophysiological stability at rest and during periods of increased cardiovascular demand. Imaging of the cardiac sympathetic system is an area of active investigation in a wide variety of conditions, such as heart failure, arrhythmias, and ischemic heart diseases, providing an independent ability to risk stratify and a potential guide for improving patient management. ^{123}I-metaiodobenzylguanidine (MIBG), an analog of the false neurotransmitter guanethidine, represents the most widely studied tracer for imaging of the cardiac autonomic system. Myocardial scintigraphy with ^{123}I-MIBG is widely used in Europe and Japan but to date there is no established standard for tracer administration, imaging acquisition, and interpretation. We discuss the current literature regarding methods and interpretation of ^{123}I-MIBG cardiac innervation imaging.

Keywords Cardiac innervation · ^{123}I-MIBG · Scintigraphy · SPECT imaging

✉ T. Pellegrino
teresa.pellegrino@ibb.cnr.it

[1] Institute of Biostructure and Bioimaging, National Council of Research, Naples, Italy

[2] Department of Advanced Biomedical Sciences, University Federico II, Naples, Italy

[3] Department of Translational Medical Sciences, University Federico II, Naples, Italy

Introduction

Cardiac autonomic sympathetic nervous system plays a relevant role in maintaining hemodynamic and electrophysiological stability at rest and in response to changing demands. As cardiac autonomic function involves several molecular processes, imaging with radionuclide tracers represents an ideal method to assess its function that is affected in a wide variety of cardiac conditions, including heart failure, arrhythmias, and ischemic heart diseases. Currently, cardiac sympathetic innervation imaging focuses on the synaptic junction and most of the developed radiotracers image pre-synaptic anatomy and function.

Myocardial scintigraphy with ^{123}I-metaiodobenzylguanidine (MIBG) is one of the few methods available for the evaluation of cardiac sympathetic functions at a clinical level. ^{123}I-MIBG is an analog of neurotransmitter norepinephrine (NE), which was developed as a sympathetic nerve-imaging agent [1]. MIBG and NE, whose chemical structures are shown in Fig. 1, have the same mechanisms for uptake, storage, and release. The uptake-1 mechanism represents the core mechanism for MIBG uptake into sympathetic nerve endings [2]. In addition, it has been reported that MIBG is stored mainly in NE storage vesicles [3], and released via exocytosis [4]. Unlike NE, MIBG is neither catabolized by monoamine oxidase or catechol-*o*-methyltransferase [5, 6]. MIBG reflects sympathetic activity at a pre-synaptic level and its role as an imaging agent to evaluate the local state of denervation and the degree of sympatheticotonia has been extensively demonstrated. This narrative review focuses on the available literature regarding methods and interpretation of ^{123}I-MIBG cardiac innervation imaging and the opportunities for further research it might suggest.

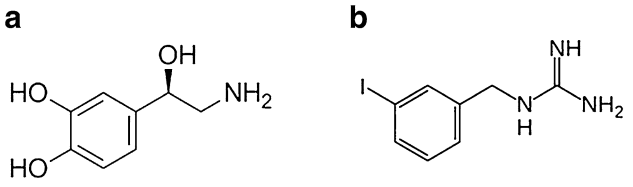

Fig. 1 Chemical structures of norepinephrine (**a**) and metaiodobenzylguanidine (**b**)

Imaging methods

Patient preparation

Although myocardial scintigraphy with ^{123}I-MIBG is largely used there are not yet accepted guidelines for tracer administration and imaging procedures. Flotats et al. [7] proposed some recommendations for standardization. To block the thyroid uptake of unbound radionuclide iodine impurities, they suggested the oral administration of potassium perchlorate (500 mg for adults, body weight-adjusted for children), or potassium iodide solution, or Lugol solution at least 30 min before ^{123}I-MIBG injection. However, there are differing views regarding pre-test administration of thyroid blocking agents. With the modern production methods the amount of impurities is minimal (i.e., <1–2 %) [8]. Friedman et al. [9] found that there was no statistical difference in the thyroid uptake between subjects receiving blockade medication compared to those not undergoing pre-treatment. More recently, Giubbini et al. [10] reported similar results in patients studied for cardiac or neurological disorders in three different centers in Italy. They found no significant differences both in tracer washout from the thyroid or 4-h thyroid-to-mediastinum ratio between patients pre-treated or not by thyroid blocking agents [10]. These findings suggest that there is a certain amount of uptake that cannot be prevented, supposedly due to ^{123}I-MIBG uptake in thyroid sympathetic nerve terminals rather than uptake of free iodine. In a previous study, Melander et al. [11] pointed out that the noradrenaline released from inter-follicular adrenergic nerve terminals has a stimulatory influence of the sympathetic nervous system on the secretion of thyroid hormone and that there was an age-related reduction of the sympathetic innervation in human thyroid tissue. Giubbini et al. [10] demonstrated that ^{123}I-MIBG thyroid uptake is lower in patients with neurological disorders than in those with cardiac diseases. Tipre et al. [12] and Matsui et al. [13] showed that sympathetic nervous denervation, and consequently reduced ^{123}I-MIBG uptake, is present in the heart but also in extra-cardiac tissues, such as thyroid, in Parkinson's disease. In addition, possible iodine allergy after administration of potassium iodide solution or Lugol solution should be considered. Many authors consider pre-treatment not necessary or without purpose, particularly in elderly patients with multiple co-morbidities or a possible iodine allergy and, therefore, its use is based on local and institutional regulations. Numerous drugs are known or may be expected to interfere with organ ^{123}I-MIBG uptake. Many studies highlighted that it is possible to perform ^{123}I-MIBG cardiac imaging in patients on optimal medical therapy (including beta-blockers, angiotensin-converting enzyme inhibitors and/or angiotensin receptor blockers) without withdraw these medications before imaging [14–16]. On the other hand, there are some medications and substances (such as food containing vanillin and catecholamine-like compounds, e.g., chocolate and blue cheese) that could interfere with the uptake of ^{123}I-MIBG [14–16] by several mechanisms (Table 1) and should be discontinued prior scan [17–19].

Tracer administration

^{123}I-MIBG should be administered by slow (over 1–2 min) secure peripheral intravenous injection flushed with saline; administered activity, in the resting condition, in an adult patient of normal body weight for a study on a multiple-head camera is in the range from 111 to 370 MBq. Adverse reactions to ^{123}I-MIBG are uncommon; administration too quickly can lead to the onset of palpitations, shortness of breath, heat sensations, transient hypertension and abdominal cramps, and an anaphylactic reaction is rare.

Image acquisition

Ten-minutes planar images of the thorax in standard anterior view are performed 15 min ("early" image) and 3–4 h ("late" image) after ^{123}I-MIBG administration with patient in the same supine position and the images are stored in a 128 × 128 or 256 × 256 matrix. Zoom should be applied, if large field-of-view cameras are used. Single-photon emission computed tomography (SPECT) studies using single- and dual-detector systems (in a 90° configuration) should be performed utilizing a rotation of 180°, starting at 45° right anterior oblique projection and proceeding anticlockwise to the 45° left posterior oblique projection. For triple-head cameras, a 360° configuration is used. SPECT images are stored in a 64 × 64 matrix. Usually, 64 projections over 180° or 128 projections over 360° are recommended, similarly to myocardial perfusion SPECT imaging [20]. The energy window is usually centered to 20 % of the 159 keV ^{123}I photo-peak. Low-energy general purpose or low-energy high-resolution (LEHR) collimators are the most commonly used, although several studies have demonstrated that medium energy (ME) collimators provide superior semi-quantitative accuracy [7, 21–23]. This is because ^{123}I has a predominant energy

Table 1 Medications that could interfere with MIBG uptake, recommended withdrawal time, and known or expected mechanism of interference

Medications	Withdrawal time	Mechanism of interference
Combined α/β-blocker	72 h	Inhibition of sodium-dependent uptake system
		Depletion of content from storage granules
Adrenergic neuron blockers	48 h	Inhibition of uptake by active transport into vesicles
		Depletion of content from storage granules
α-Blocker	15 days	Unknown mechanisms
Calcium channel blockers	24–48 h	Calcium-mediated
		Unknown mechanisms
Isotropic sympathomimetics	24 h	Depletion of content from storage granules
Vasoconstrictor sympathomimetics	24 h	Inhibition of sodium-dependent uptake system
		Depletion of content from storage granules
β_2 Stimulants	24 h	Depletion of content from storage granules
Systemic and local nasal decongestants, compound cough	24–48 h	Inhibition of sodium-dependent uptake system
		Depletion of content from storage granules
Sympathomimetics for glaucoma	48 h	Depletion of content from storage granules
Neuroleptics	24–72 h to 15 days	Inhibition of sodium-dependent uptake system
Sedating antihistamines	24 h	Inhibition of sodium-dependent uptake system
Opioid analgesics	24 h	Inhibition of sodium-dependent uptake system
Tryciclic antidepressants	24–48 h	Inhibition of sodium-dependent uptake system
Central nervous system stimulants	24–48 h to 5 days	Inhibition of sodium-dependent uptake system
		Depletion of content from storage granules
		Unknown mechanisms

emission of 159 keV (97 %), that is optimal imaging energy in nuclear medicine, but it also emits high-energy photons >400 keV (3 %) which penetrate the LEHR collimator thin septa (0.16–0.3 mm) and cause multiple Compton scatter photons that increase the background noise around the main 159 keV energy peak. This leads to image blurring and underestimation of myocardial counts compared to the outside regions. The increased septal thickness (1 mm) of ME collimators increases the image resolution minimizing scatter in the images obtaining superior image contrast of the myocardium to background [7, 21–23]. In Europe and US most laboratories use LEHR collimators without any scatter correction, whereas in Japan the low-medium energy collimators are more widely used. Some studies have proposed several scatter compensation methods [24–28] to offset for the resulting corruption of image related to the use of LEHR collimator due to penetration by higher energy photons. Recently, Chen et al. [28, 29] developed a deconvolution of septal penetration technique, a mathematical method that optimizes acquisition and processing protocols obtaining similar results for LEHR and medium energy all-purpose collimators. The authors concluded that this technique seems to improve quantitative accuracy of ^{123}I cardiac SPECT imaging in reference to a phantom standard. Phantom calibration for each center performing MIBG imaging may be very beneficial and is also less complicated than the development of site-specific normal limits. However, the usefulness of phantom calibration approach in clinical applications has yet to be determined. Nakajima et al. [30] suggested that a phantom calibration should be used to calibrate the results obtained by ME and LEHR collimators. The same authors also recently reported the results of a multi-center study about cross-institution phantom calibrations for the analysis of heart-to-mediastinum (H/M) ratio by standard camera from various vendors and collimators [31]. The study demonstrated a significant variability in H/M ratios between ME and LEHR collimators, but also within the same collimator from different vendors, because they can have some different characteristics [31]. For example, for the H/M reference value of 1.6, used as a threshold in risk stratification [32], the measured H/M ratios ranged between 1.54 and 2.06 (95 % lower–upper range), depending on the site when both low energy and ME collimators are included. To overcome this issue, it has been suggested that the H/M ratio threshold of 1.6 reported with the LEHR collimator should be converted to 2.0 for an institution in which the ME general-purpose collimator is used [33]. However, differences in the software used for analysis and variability in defining the regions of interest for mediastinum or heart may impact the result observed, especially in subjects with abnormal studies [34].

SPECT reconstruction methods

Currently two different reconstruction methods are available: the analytical and the iterative method. The first is represented by filtered back-projection that uses a ramp filter in conjunction with a low-pass filter (Hanning or Butterworth) in order to minimize the high spatial frequency components of the image decreasing the noise. The iterative methods are represented by the maximum likelihood expectation maximization (MLEM) and the ordered subsets expectation maximization (OSEM). Frequently, 10–15 iterations for MLEM and 2 iterations for OSEM are recommended. The reconstructed transaxial data are then reoriented into three standard image planes. Several automated methods for reorientation are available [35, 36]. However these methods may fail in patients with large defects of cardiac tracer uptake.

Imaging analysis

The analysis of planar ^{123}I-MIBG cardiac imaging includes the semi-quantitative analysis of global uptake by calculating early and late H/M ratios and the rate of the tracer that is washed out from the myocardium in the interval between early and late acquisitions, by calculating the washout rate (Fig. 2). The semi-quantitative analysis is obtained by calculating the H/M ratio on early and late images [37, 38] after drawing regions of interest (ROI) over the entire heart and upper mediastinum. Ideally, the mediastinal ROI is a predefined a square (7 × 7 pixels) placed on the upper half of the mediastinum. The location of the mediastinal ROI is determined using the lung apex, the upper cardiac border, and the medial contours of the lungs as landmarks. Care must be taken to exclude lung or liver from the myocardial and large vessels and lung from the mediastinum region of interest. The H/M ratios are computed from early and late planar images by dividing the mean counts per pixel within the myocardium by the mean counts per pixel within the mediastinum [39]. Washout rate, expressed as a percentage, is calculated using the following formula: [(early heart counts/pixel − early mediastinum counts/pixel) − (late heart counts/pixel decay-corrected − late mediastinum counts/pixel decay-corrected)]/(early heart counts/pixel − early mediastinum counts/pixel) × 100. The time decay correction factor is $1/0.5^{t/13}$ for time t (h), and if the interval between the scans is 3 h, then the correction factor is 1.17 [33].

On SPECT images regional uptake of the tracer is usually assessed by visual review. The total defect score is calculated by assessing the patient's segmental tracer uptake score using the 17-segment model (Fig. 3). Each myocardial segment is scored according to the following tracer uptake scale: 0 normal, 1 mildly reduced, 2 moderately reduced, 3 severely reduced, and 4 no uptake. Individual myocardial segments can be assigned to the three major coronary arteries (left anterior descending artery, left circumflex artery, and right coronary artery) according to the recommendation of the American Heart Association [40], with the recognition that there is anatomic variability. The defect scores are calculated as the sum of the segmental tracer uptake scores (summed score) and separately for each vascular territory.

Methods for analyses remain under investigation. Techniques are being explored to standardize the H/M ratio. Okuda et al. [41] proposed an automatic algorithm that determines the mediastinal ROI based on tracer uptake in the heart, lung, liver, and thyroid. However, few data are available on the reproducibility of this technique [39, 42]. Recently, we demonstrated a high observer reproducibility of planar H/M ratios and SPECT defect scores using a low-

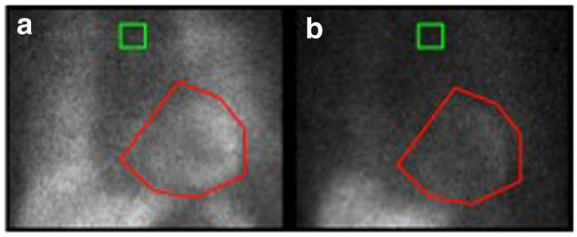

$$\text{H/M} = \frac{\text{heart counts/pixel}}{\text{mediastinum counts/pixel}}$$

$$\text{WR} = \frac{[(\text{early H counts/pixel} - \text{early M counts/pixel}) - (\text{late H counts/pixel}^* - \text{late M counts/pixel}^*)]}{(\text{early H counts/pixel} - \text{early M counts/pixel})} \times 100$$

*decay corrected

Fig. 2 Planar ^{123}I-metaiodobenzylguanidine imaging with calculation of heart-to-mediastinum ratio and washout rate after drawing regions of interest over the heart (*red line*) and mediastinum (*green line*). *H/M* heart-to-mediastinum; *WR* washout rate

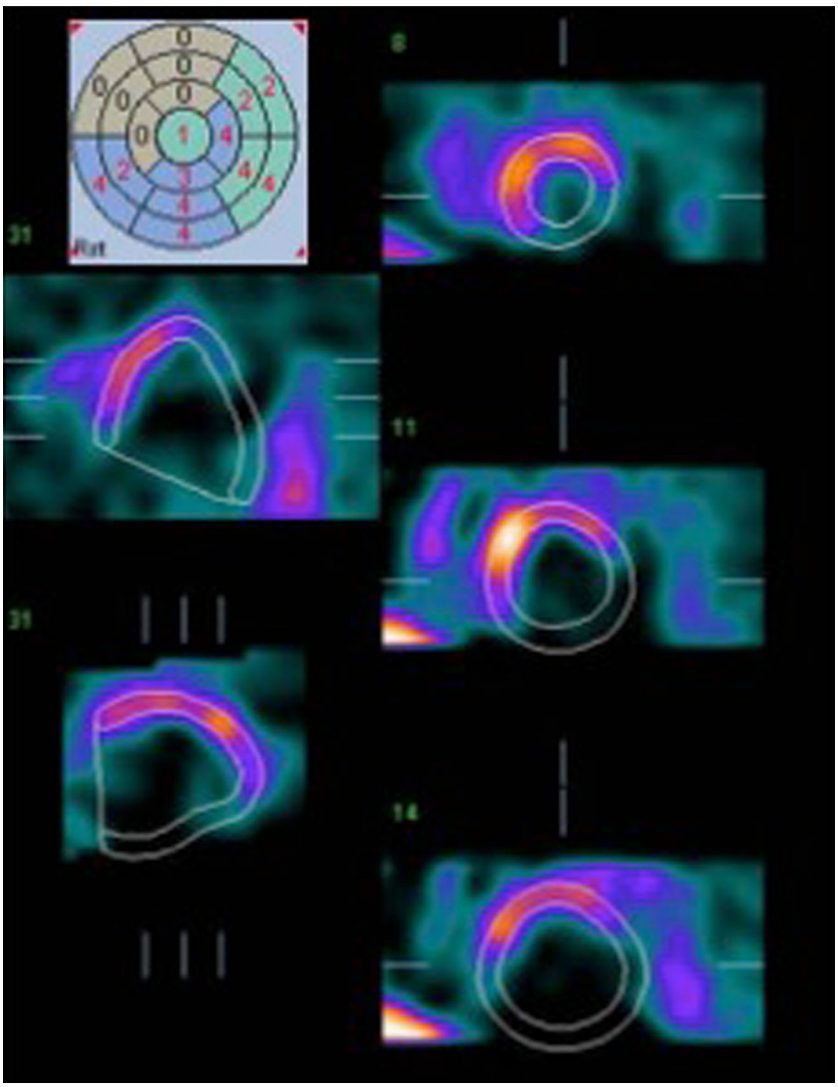

Fig. 3 Single-photon emission computed tomography ^{123}I-metaiodobenzylguanidine imaging with construction of myocardial polar maps and assessment of innervation defect extent and severity

dose ^{123}I-MIBG cardiac imaging protocol [43]. The intra-class coefficient of correlation, Lin's concordance correlation coefficient, and Bland–Altman analysis were used to evaluate the intra- and the inter-observer reproducibility [44]. With these approaches, the differences between measurements obtained twice by the same examiner and by two examiners were negligible for both early and late H/M ratios and for SPECT defect scores. Jacobson et al. [45] highlighted that the measure of H/M ratios are not affected by the differences in manually placed ROI. Nevertheless the analysis has not yet been standardized between institutions and countries [46].

Imaging interpretation

Early ^{123}I-MIBG H/M ratio reflects the integrity of pre-synaptic nerve terminals and late H/M ratio the relative distribution of sympathetic nerve terminals, offering global information about neuronal function resulting from uptake, storage, and release. ^{123}I-MIBG washout rate reflects the neuronal integrity or sympathetic tone, mainly representing uptake-1. Interpretation of ^{123}I-MIBG SPECT is less well established, in part because of frequent poor quality of images, as well as the overlying extra-cardiac (lung and liver) activity that can obscure parts of the myocardium and the presence of regional heterogeneous ^{123}I-MIBG uptake in healthy individuals. Somsen et al. [39] showed a lower activity in the inferior than the lateral wall, probably due to anatomic variation in sympathetic nerve activity. Tsuchimochi et al. [47] demonstrated that heterogeneities might be more pronounced in men and healthy older subjects. Estorch et al. [48] highlighted that ^{123}I-MIBG uptake is reduced in the inferior wall in athletes with sinus bradycardia, probably due to increased vagal tone.

The major limitation of ^{123}I-MIBG planar and SPECT imaging techniques is that they cannot measure absolute myocardial tracer uptake. In addition, the optimal cut-off

indicating abnormal sympathetic activity and for prognostication has not yet been identified. Jacobson et al. [49] proposed a H/M ratio threshold of 1.6, based on the 95th percentile normal limits obtained in normal controls. Nakata et al. [46] recently suggested a higher threshold of 1.68 in a multi-center study using LEHR collimators. Anyway the use of binary thresholds should be considered with caution since it may cause misclassification of a large percentage of cases which are close to the binary threshold creating a substantial gray-zone related to the test variability, as we recently reported [50].

Conclusions

Radionuclide autonomic imaging promises to yield information that cannot be provided by other imaging techniques. It represents an added value in identifying patient at risk of heart failure progression. It is important to promote the implementation of neuronal imaging agents for routine clinical. New scanners based on solid-state cadmium-zinc-telluride detectors have the potential to improve the ^{123}I-MIBG accuracy due to higher photon energy resolution and thus to discriminate better scattered photons. These cameras can also evaluate dynamic myocardial innervation in vivo [51]. The values of SPECT quantification schemes and of the new generation scanners need to be further validate in large prognostic studies.

Author's contribution T Pellegrino: Literature Search and Review, Manuscript Writing. M Petretta and A Cuocolo: Content planning and Editing.

Compliance with ethical standards

Conflict of interest The author declares not to have conflict of interest.

Ethical standards This article does not contain any studies with human or animal subjects performed by any of the Authors.

References

1. Wieland DM, Wu J, Brown LE, Mangner TJ, Swanson DP, Beierwaltes WH (1980) Radiolabeled adrenergic neuron-blocking agents: adrenomedullary imaging with [131I] iodobenzylguanidine. J Nucl Med 21:349–353
2. Tobes MC, Jaques S Jr, Wieland DM, Sisson JC (1985) Effect of uptake-one inhibitors on the uptake of norepinephrine and metaiodobenzylguanidine. J Nucl Med 26:897–907
3. Nakajo M, Shimabukuro K, Yoshimura H, Yonekura R, Nakabeppu Y, Tanoue P, Shinohara S (1986) Iodine-131 metaiodobenzylguanidine intra and extravesicular accumulation in the rat heart. J Nucl Med 27:84–89
4. Sisson JC, Wieland DM, Sherman P, Mangner TJ, Tobes MC, Jacques S Jr (1987) Metaiodobenzylguanidine as an index of the adrenergic nervous system integrity and function. J Nucl Med 28:16201624
5. Wieland DM, Brown LE, Tobes MC, Rogers WL, Marsh DD, Mangner TJ, Swanson DP, Beierwaltes WH (1981) Imaging the primate adrenal medulla with [123I] and [131I] meta-iodobenzylguanidine: concise communication. J Nucl Med 22:358–364
6. Wieland DM, Brown LE, Rogers WL, Worthington KC, Wu JL, Clinthorne NH, Otto CA, Swanson DP, Beierwaltes WH (1981) Myocardial imaging with a radioiodinated norepinephrine storage analog. J Nucl Med 22:22–31
7. Flotats A, Carrió I, Agostini D, Le Guludec D, Marcassa C, Schäfers M, Somsen GA, Unlu M, Verberne HJ, EANM Cardiovascular Committee, European Council of Nuclear Cardiology (2010) Proposal for standardization of 123I-metaiodobenzylguanidine (MIBG) cardiac sympathetic imaging by the EANM Cardiovascular Committee and the European Council of Nuclear Cardiology. Eur J Nucl Med Mol Imaging 37:1802–1812
8. Vallabhajosula S, Nikolopoulou A (2011) Radioiodinated metaiodobenzylguanidine (MIBG): radiochemistry, biology, and pharmacology. Semin Nucl Med 41:324–333
9. Friedman NC, Hassan A, Grady E, Matsuoka DT, Jacobson AF (2014) Efficacy of thyroid blockade on thyroid radioiodine uptake in 123I-mIBG imaging. J Nucl Med 55:211–215
10. Giubbini R, Milan E, Marcassa C, Paghera B, Fracassi F, Camoni L, Rodella C, Bertagna F, Motta F, Bertoli M, Campini R (2015) 1-23I-MIBG thyroid uptake: implications for MIBG imaging of the heart. J Nucl Cardiol **[Epub ahead of print]**
11. Melander A, Ljunggren JG, Norberg KA, Persson B, Rosengren E, Sundler F, Tibblin S, Westgren U (1978) Sympathetic innervation and noradrenaline content of normal human thyroid tissue from fetal, young, and elderly subjects. J Endocrinol Invest 1:175–177
12. Tipre DN, Goldstein DS (2005) Cardiac and extracardiac sympathetic denervation in Parkinson's disease with orthostatic hypotension and in pure autonomic failure. J Nucl Med 46:1775–1781
13. Matsui H, Udaka F, Oda M, Tamura A, Kubori T, Nishinaka K, Kameyama M (2005) Metaiodobenzylguanidine (MIBG) uptake in Parkinson's disease also decreases at thyroid. Ann Nucl Med 19:225–229
14. Yamashina S, Yamazaki J (2007) Neuronal imaging using SPECT. Eur J Nucl Med Mol Imaging 34(Suppl 1):S62–S73
15. Agostini D, Carrio I, Verberne HJ (2009) How to use myocardial 123I-MIBG scintigraphy in chronic heart failure. Eur J Nucl Med Mol Imaging 36:555–559
16. Carrió I, Cowie MR, Yamazaki J, Udelson J, Camici PG (2010) Cardiac sympathetic imaging with mIBG in heart failure. JACC Cardiovasc Imaging 3:92–100
17. Solanki KK, Bomanji J, Moyes J, Mather SJ, Trainer PJ, Britton KE (1992) A pharmacological guide to medicines which interfere with the biodistribution of radiolabelled meta-iodobenzylguanidine (MIBG). Nucl Med Commun 13:513–521
18. Wafelman AR, Hoefnagel CA, Maes RA, Beijnen JH (1994) Radioiodinated metaiodobenzylguanidine: a review of its biodistribution and pharmacokinetics, drug interactions, cytotoxicity and dosimetry. Eur J Nucl Med 21:545–559
19. Jacobson AF, Travin MI (2015) Impact of medications on mIBG uptake, with specific attention to the heart: comprehensive review of the literature. J Nucl Cardiol 22(5):980–993
20. Hesse B, Tägil K, Cuocolo A, Anagnostopoulos C, Bardiés M, Bax J, Bengel F, Busemann Sokole E, Davies G, Dondi M, Edenbrandt L, Franken P, Kjaer A, Knuuti J, Lassmann M, Ljungberg M, Marcassa C, Marie PY, McKiddie F, O'Connor M, Prvulovich E, Underwood R, van Eck-Smit B, EANM/ESC Group (2005) EANM/ESC procedural guidelines for myocardial

perfusion imaging in nuclear cardiology. Eur J Nucl Med Mol Imaging 32:855–897
21. Verberne HJ, Feenstra C, de Jong WM, Somsen GA, van Eck-Smit BL, Busemann Sokole E (2005) Influence of collimator choice and simulated clinical conditions on 123I-MIBG heart/mediastinum ratios: a phantom study. Eur J Nucl Med Mol Imaging 32:1100–1107
22. Dobbeleir AA, Hambÿe AS, Franken PR (1999) Influence of high-energy photons on the spectrum of iodine-123 with low- and medium-energy collimators: consequences for imaging with 123I-labelled compounds in clinical practice. Eur J Nucl Med 26:655–658
23. Inoue Y, Suzuki A, Shirouzu I, Machida T, Yoshizawa Y, Akita F, Ohnishi S, Yoshikawa K, Ohtomo K (2003) Effect of collimator choice on quantitative assessment of cardiac iodine 123 MIBG uptake. J Nucl Cardiol 10:623–632
24. Jaszczak RJ, Greer KL, Floyd CE Jr, Harris CC, Coleman RE (1984) Improved SPECT quantification using compensation for scattered photons. J Nucl Med 25:893–900
25. Koral KF, Wang XQ, Rogers WL, Clinthorne NH, Wang XH (1988) SPECT Compton-scattering correction by analysis of energy spectra. J Nucl Med 29:195–202
26. Gagnon D, Todd-Pokropek A, Arsenaualt A, Dupras G (1989) Introduction to holospectral imaging in nuclear medicine for scatter subtraction. IEEE Trans Med Imaging 8:245–250
27. Haynor DR, Kaplan MS, Miyaoka RS, Lewellen TK (1995) Multiwindow scatter correction techniques in single-photon imaging. Med Phys 22:2015–2024
28. Chen J, Garcia EV, Galt JR, Folks RD, Carrio I (2006) Optimized acquisition and processing protocols for I-123 cardiac SPECT imaging. J Nucl Cardiol 13:251–260
29. Chen J, Garcia EV, Galt JR, Folks RD, Carrio I (2006) Improved quantification in 123I cardiac SPECT imaging with deconvolution of septal penetration. Nucl Med Commun 27:551–558
30. Nakajima K, Okuda K, Matsuo S, Yoshita M, Taki J, Yamada M, Kinuya S (2012) Standardization of metaiodobenzylguanidine heart to mediastinum ratio using a calibration phantom: effects of correction on normal databases and a multicentre study. Eur J Nucl Med Mol Imaging 39:113–119
31. Nakajima K, Okuda K, Yoshimura M, Matsuo S, Wakabayashi H, Imanishi Y, Kinuya S (2014) Multicenter cross-calibration of I-123 metaiodobenzylguanidine heart-to-mediastinum ratios to overcome camera-collimator variations. J Nucl Cardiol 21:970–978
32. Jacobson AF, Senior R, Cerqueira MD, Wong ND, Thomas GS, Lopez VA, Agostini D, Weiland F, Chandna H, Narula J, Investigators ADMIRE-HF (2010) Myocardial iodine-123 metaiodobenzylguanidine imaging and cardiac events in heart failure. Results of the prospective ADMIRE-HF (AdreView Myocardial Imaging for Risk Evaluation in Heart Failure) study. J Am Coll Cardiol 55:2212–2221
33. Nakajima K, Nakata T (2015) Cardiac 123I-MIBG imaging for clinical decision making: 22-year experience in Japan. J Nucl Med 56(Suppl 4):11S–19S
34. Slomka PJ, Mehta PK, Germano G, Berman DS (2014) Quantification of I-123-meta-iodobenzylguanidine heart-to-mediastinum ratios: not so simple after all. J Nucl Cardiol 21:979–983
35. Germano G, Kavanagh PB, Chen J, Waechter P, Su HT, Kiat H, Berman DS (1995) Operator-less processing of myocardial perfusion SPECT studies. J Nucl Med 36:2127–2132
36. Slomka PJ, Hurwitz GA, Stephenson J, Cradduck T (1995) Automated alignment and sizing of myocardial stress and rest scans to three-dimensional normal templates using an image registration algorithm. J Nucl Med 36:1115–1122
37. Merlet P, Valette H, Dubois-Randé JL, Moyse D, Duboc D, Dove P, Bourguignon MH, Benvenuti C, Duval AM, Agostini D, Loisance D, Castaigne A, Syrota A (1992) Prognostic value of cardiac metaiodobenzylguanidine imaging in patients with heart failure. J Nucl Med 33:471–477
38. Estorch M, Carrió I, Berná L, López-Pousa J, Torres G (1995) Myocardial iodine-labeled metaiodobenzylguanidine 123 uptake relates to age. J Nucl Cardiol 2:126–132
39. Somsen GA, Verberne HJ, Fleury E, Righetti A (2004) Normal values and within-subject variability of cardiac I-123 MIBG scintigraphy in healthy individuals: implications for clinical studies. J Nucl Cardiol 11:126–133
40. Cerqueira MD, Weissman NJ, Dilsizian V, Jacobs AK, Kaul S, Laskey WK, Pennell DJ, Rumberger JA, Ryan T, Verani MS, American Heart Association Writing Group on Myocardial Segmentation and Registration for Cardiac Imaging (2002) Standardized myocardial segmentation and nomenclature for tomographic imaging of the heart. A statement for healthcare professionals from the Cardiac Imaging Committee of the Council on Clinical Cardiology of the American Heart Association. Circulation 105:539–542
41. Okuda K, Nakajima K, Hosoya T, Ishikawa T, Konishi T, Matsubara K, Matsuo S, Kinuya S (2011) Semi-automated algorithm for calculating heart-to-mediastinum ratio in cardiac iodine-123 MIBG imaging. J Nucl Cardiol 18:82–89
42. Veltman CE, Boogers MJ, Meinardi JE, Al Younis I, Dibbets-Schneider P, Van der Wall EE, Bax JJ, Scholte AJ (2012) Reproducibility of planar (123)I-meta-iodobenzylguanidine (MIBG) myocardial scintigraphy in patients with heart failure. Eur J Nucl Med Mol Imaging 39:1599–1608
43. Pellegrino T, Petretta M, De Luca S, Paolillo S, Boemio A, Carotenuto R, Petretta MP, di Nuzzo C, Perrone-Filardi P, Cuocolo A (2013) Observer reproducibility of results from a lowdose 123I-metaiodobenzylguanidine cardiac imaging protocol in patients with heart failure. Eur J Nucl Med Mol Imaging 40:1549–1557
44. de Vet HC, Terwee CB, Knol DL, Bouter LM (2006) When to use agreement versus reliability measures. J Clin Epidemiol 59:1033–1039
45. Jacobson AF, Matsuoka DT (2013) Influence of myocardial region of interest definition on quantitative analysis of planar 123I-mIBG images. Eur J Nucl Med Mol Imaging 40:558–564
46. Nakata T, Nakajima K, Yamashina S, Yamada T, Momose M, Kasama S, Matsui T, Matsuo S, Travin MI, Jacobson AF (2013) A pooled analysis of multicenter cohort studies of (123)I-mIBG imaging of sympathetic innervation for assessment of long-term prognosis in heart failure. JACC Cardiovasc Imaging 6:772–784
47. Tsuchimochi S, Tamaki N, Tadamura E, Kawamoto M, Fujita T, Yonekura Y, Konishi J (1995) Age and gender differences in normal myocardial adrenergic neuronal function evaluated by iodine-123-MIBG imaging. J Nucl Med 36:969–974
48. Estorch M, Serra-Grima R, Flotats A, Marí C, Bernà L, Catafau A, Martín JC, Tembl A, Narula J, Carrió I (2000) Myocardial sympathetic innervation in the athlete's sinus bradycardia: is there selective inferior myocardial wall denervation? J Nucl Cardiol 7:354–358
49. Jacobson AF, Lombard J, Banerjee G, Camici PG (2009) 123I-mIBG scintigraphy to predict risk for adverse cardiac outcomes in heart failure patients: design of two prospective multicenter international trials. J Nucl Cardiol 16:113–121
50. Petretta M, Pellegrino T, Cuocolo A (2014) The "gray zone" for the heart to mediastinum MIBG uptake ratio. J Nucl Cardiol 21:921–924
51. Giorgetti A, Burchielli S, Positano V, Kovalski G, Quaranta A, Genovesi D, Tredici M, Duce V, Landini L, Trivella MG, Marzullo P (2015) Dynamic 3D analysis of myocardial sympathetic innervation: an experimental study using 123I-MIBG and a CZT camera. J Nucl Med 56:464–469